The AURORA Survey: A New Era of Emission-line Diagrams with *JWST*/NIRSpec

Alice E. Shapley,[1] Ryan L. Sanders,[2] Michael W. Topping,[3] Naveen A. Reddy,[4] Danielle A. Berg,[5] Rychard J. Bouwens,[6] Gabriel Brammer,[7] Adam C. Carnall,[8] Fergus Cullen,[8] Romeel Davé,[8] James S. Dunlop,[8] Richard S. Ellis,[9] N. M. Förster Schreiber,[10] Steven R. Furlanetto,[1] Karl Glazebrook,[11] Garth D. Illingworth,[12] Tucker Jones,[13] Mariska Kriek,[6] Derek J. McLeod,[8] Ross J. McLure,[8] Desika Narayanan,[14] Pascal Oesch,[15] Anthony J. Pahl,[16] Max Pettini,[17] Daniel Schaerer,[15] Daniel P. Stark,[3] Charles C. Steidel,[18] Mengtao Tang,[3] Leonardo Clarke,[1] Callum T. Donnan,[8] and Emily Kehoe[1]

Introduction

Recombination and collisionally-excited emission lines from star-forming regions
→interplay between massive stars, gas, dust, and heavy elements in the ionized ISM
rest-optical emission line properties of star-forming galaxies at $z \sim 2-3$
→photoionization by chemically-young massive stars
AURORA *JWST*/NIRSpec program : detect faint auroral lines from ionized O, S, and N for $z > 1.4$ galaxies
→direct chemical abundances
- high S/N measurements of emission-line ratio diagrams for individual high-z galaxies
- rest-frame blue-optical emission-line diagnostics for $z > 10$ spectra
- first statistical sample of rest-frame near-IR diagnostics for star-forming galaxies at $z > 1$

Observations

AURORA NIRSpec observations : COSMOS field and GOODS- N
- $R \sim 1000$ & wavelength range ~1 – 5μm

AURORA targets selection
AURORA sample of 97
→measured redshifts and emission-line fluxes for 95 galaxies (Figure 1)
→identify star-forming galaxies by removing AGNs and quiescent galaxies
→several emission-line-ratio diagrams of 87 of star-forming galaxies (z=1.4-7.5)

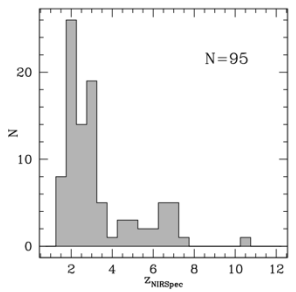

Figure 1. AURORA redshift distribution. This distribution includes

comparison with z~0 galaxies and H II regions
- z~0 galaxies : SDSS DR7, MaNGA for relationship between [OIII]λ5007 and [SIII]/[SII]
- H II regions : CHAOS survey (DIG-free)
- SDSS emission-line spectra of $z \sim 0$ galaxies include the contributions of both H II regions and diffuse ionized gas (DIG)
  ⇨emission-line ratio diagrams include [OI] and [SII] emission were compared with local H II regions

Results & Discussion

Classical emission-line diagrams

- BPT diagrams (Figure 4)
  - higher [NII]λ6583/Hα and [OIII]λ5007/Hβ than $z \sim 0$ star-forming galaxies
  - higher [OIII]λ5007/Hβ, [SII]λλ6717, 6731/Hα, and [OI]λ6300/Hα than local H II regions
  ⇨photoionization by harder ionizing spectrum at fixed nebular metallicity than low-z star-forming galaxies
  - $z = 2.7-4.0$ sample is further offset from the $z \sim 0$ sequence than the $z = 1.4-2.7$ sample in [NII] diagram
    - target redshift distribution is skewed to $z = 1.4-4$
    ⇨larger sample of $z \sim 4-6.5$ with the same wavelength coverage and comparable depth are required
  - typical [NII]λ6583/Hα line ratios ($M_* = 10^8 - 10^{10} M_\odot$, z>4) : 0.03-0.06 (e.g. Shapley et al. 2023b)
    ↔large dynamic range in [NII]λ6583/Hα, even at $z > 6$ (AURORA)
    ⇨ require much larger samples in [NII] BPT diagram at $z > 4$

- [OIII]λ5007/[OII]λ3727 (O32) vs. ([OII]λ3727+[OIII]λλ4959, 5007)/Hβ (R23) (Figure 5)
  - to investigate the combination of ionization parameter and metallicity in star-forming galaxies
  - higher average *O*32 at increasing redshift
  - 20 galaxies with log(*R*23) ≥ 1
    - virtually no corresponding measurements of local star-forming galaxies at high log(*R*23) values
  - hardening the ionizing spectrum at fixed nebular metallicity in photoionization models produces higher peak *R*23 values at fixed *O*32 in photoionization models
    ⇨detail photoionization modeling of the ionization parameter and ionizing spectrum of individual galaxies with direct metallicity estimates are required

Results & Discussion

Emission-line diagnostic diagram based on bluer rest-frame optical features (Figure 6)

- to understand the physical properties of the ISM in high-z galaxies
- in space of ionization and metallicity
  - [NeIII]λ3869/[OII]λ3727 ratio serves as *O*32
  - ([NeIII]λ3869+[OII]λ3727)/Hδ serves as *R*23
- overlap with the high [NeIII]λ3869/[OII]λ3727, low ([NeIII]λ3869+[OII]λ3727)/Hδ tail of $z \sim 0$ distribution
- higher [NeIII]λ3869/[OII]λ3727 and lower ([NeIII]λ3869+[OII]λ3727)/Hδ at increasing redshift
  - GN-z11 and the $z \sim 5.5-9.5$ stacks are consistent with the $z > 5$ of the AURORA sample
- exception : auroral target GOODSN-30274 ($z = 1.800$, red) & filler target GOODSN-917107 ($z = 4.773$, blue)
  - similar line ratios with GN-z11
  →insights into the detailed nature of GN-z11

Emission- line diagnostic diagram based on longer wavelength

- [SIII]λλ9069,9532/[SII]λλ6717,6731 (*S*32) (Figure7)
  - probe of the ionization parameter and ionization state of the ISM in $z \sim 0$ galaxies
  - differentiate between the effects of an evolving ionizing spectrum or ionization parameter at fixed nebular metallicity in high-z star-forming regions with the [OIII]λ5007/Hβ ratio
  - offset from local H II regions
  - towards lower *S*32 at fixed [OIII]λ5007/Hβ
    ⇨harder ionizing spectrum at fixed nebular metallicity

- rest-frame near-IR line ratios (Figure 8)
  - recent *JWST* works on rest-frame near-IR emission lines in distant galaxies feature [FeII]λ1.257μm/Paβ ratio
    - pair with He Iλ1.083μm/Paγ (Brinchmann 2023) or [SIII]λ9532/Paγ (Calabrò et al. 2023)
  - compare with Cloudy photoionization models (Ferland et al. 2017)
    - a dust depletion factor of 20 for Fe
  - AURORA sample can be explained by photoionization by massive stars
    - median [FeII]λ1.257μm/Paβ is 0.2 (corresponds to [FeII]λ1.257μm/Hβ = 0.03)
      - within the range of stellar photoionization model predictions
      - lower than sample of local starbursts (0.34) (Calzetti 1997)
        →constrain the origin of [FeII] emission in distant star-forming galaxies
  - significant systematic uncertainty between measurements and models is associated with the assumed dust depletion factor for Fe
    - better constraints on dust depletion for Fe incorporating metallicity dependence in distant star-forming galaxies are important

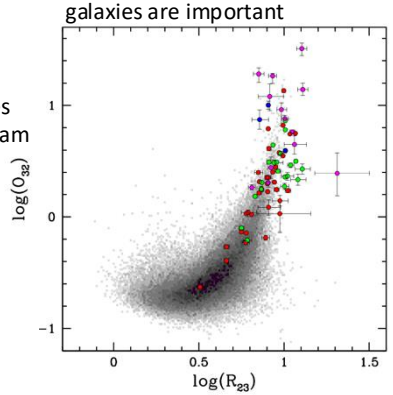

Figure 5. O_{32} vs. R_{23} diagram, corrected for dust. Symbols for

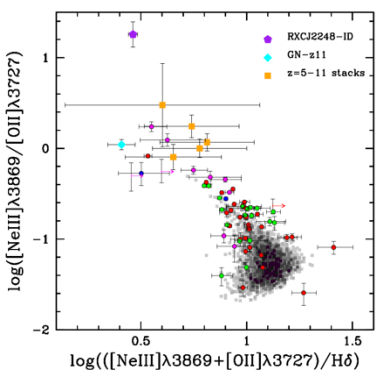

Figure 6. [NeIII]λ3869/[OII]λ3727 vs. ([NeIII]λ3869+[OII]λ3727)/Hδ, corrected for dust. Symbols

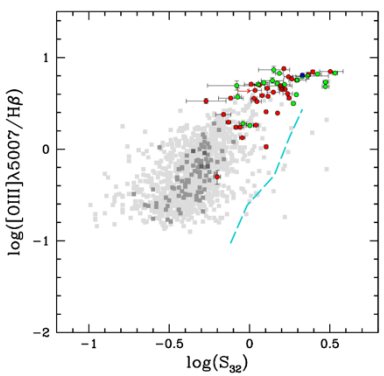

Figure 7. [OIII]λ5007/Hβ vs. S_{32} (dust-corrected). Symbols for

Conclusion

AURORA sample enabled high S/N measurements of individual high-z galaxies
→evolution of ISM and chemical enrichment
larger sample will be collected for detail interpreting the emission-line diagnostic diagrams

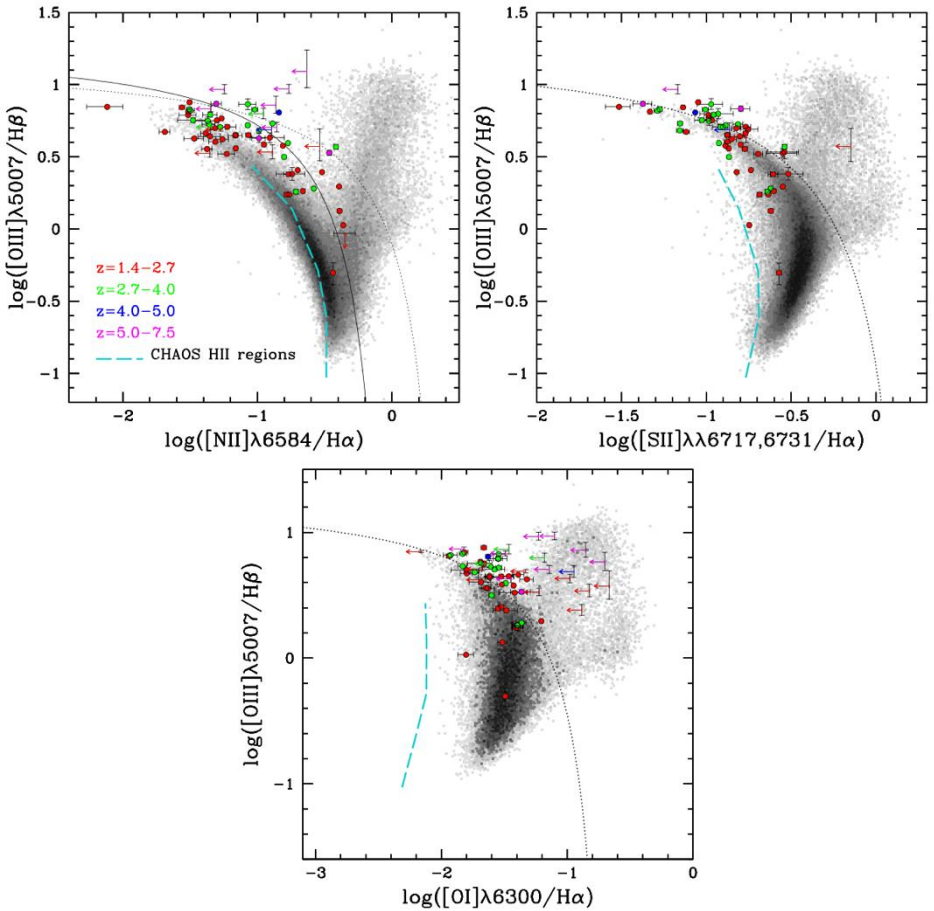

Figure 4. "Classical" Emission-line Diagnostic Diagrams. In each panel, galaxies from the AURORA sample are plotted with colored symbols.

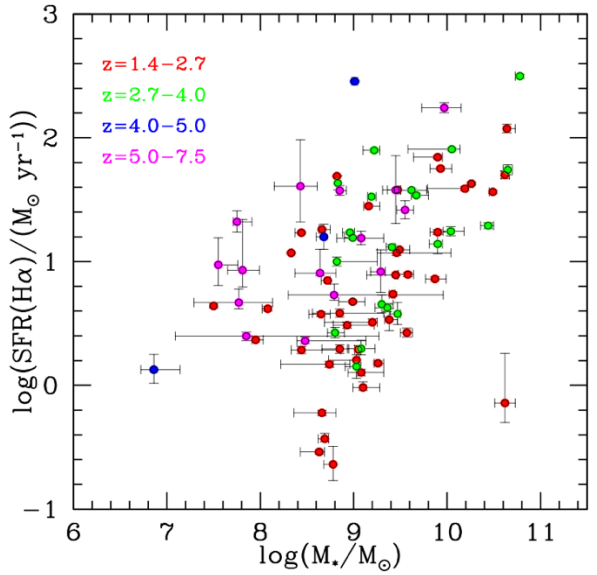

Figure 3. SFR(Hα) vs. M_*. Red, green, blue, and magenta symbols

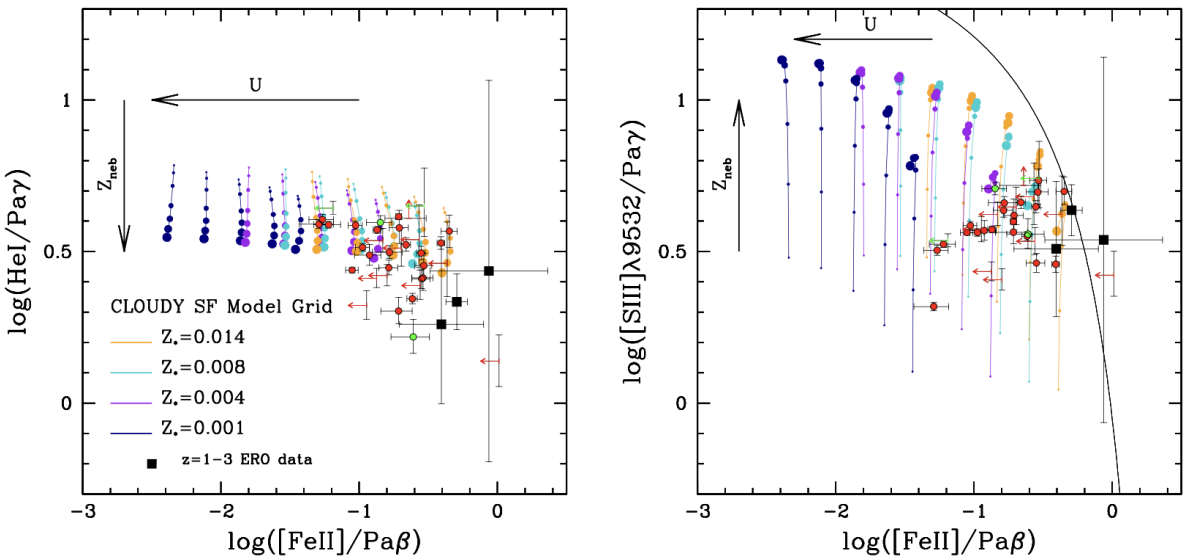

Figure 8. Rest-frame Near-IR Emission-line Ratios. Symbols for AURORA galaxies are as in Figure 4. Plotted in each panel are Cloudy